PHYSICAL REVIEW E, VOLUME 65, 051309

Probing the internal field gradients of porous media

Boqin Sun and Keh-Jim Dunn
Chevron Texaco Exploration and Production Technology Company, San Ramon, California 94583
(Received 1 October 2001; revised manuscript received 6 February 2002; published 22 May 2002)

We devise a modified Carr-Purcell-Meiboom-Gill pulse sequence that allows us to probe the apparent internal field gradient distribution of a fluid-saturated porous medium as a function of the pore size. This distribution is displayed as a two-dimensional map with one axis being the field gradient, another axis being the T_2 relaxation time reflecting different pore sizes, and the vertical amplitudes being proportional to the proton population. Such a scheme of two-dimensional representation for fluid-saturated porous media can also be used for the identification of pore fluids using the contrast of their diffusion coefficients.

DOI: 10.1103/PhysRevE.65.051309 PACS number(s): 81.05.Rm, 91.60.Pn, 76.60.Jx, 66.10.Cb

I. INTRODUCTION

In a fluid-saturated porous medium, the solid matrix or solid/fluid interface can contain paramagnetic impurities that have a magnetic susceptibility value very different from that of the fluid in the pores. When such a fluid-saturated porous sample is placed in an external, homogeneous magnetic field, this contrast in magnetic susceptibility between solid grains and pore fluid can cause significant local field inhomogeneities inside the pores [1]. While the average internal magnetic field gradient is estimated to be proportional to the susceptibility difference and the field strength and inversely proportional to the size of the pore, the detailed behavior of the internal field gradient as a function of the pore size can be much more complicated, as it also depends on the grain shape, the aspect ratio of the pore, and the microgeometry of the pore network.

The problem of the internal magnetic field gradients of porous media was treated theoretically for a single pore scale periodic system [1]. However, it has never been successfully characterized experimentally for multiple pore scale systems, such as rocks. In this paper, we show that the internal magnetic field gradient distribution of a water-saturated porous medium for a multiple pore scale disordered system can be clearly delineated by a two-dimensional (2D) plot in a semiquantitative manner.

Understanding the internal magnetic field distribution in porous media, such as rocks, is not only academically interesting, but also important with practical implications in oil exploration. If such a distribution as a function of pore size is understood quantitatively, methods can be devised to remove it or reduce its adverse effects in the analysis of the proton nuclear magnetic resonance (NMR) relaxation data obtained from borehole logging measurements. This is very important if one attempts to extract information about the properties of the pore fluids saturating the porous media from proton NMR signals distorted by the presence of internal field gradients and molecular diffusion.

In the following, we show that using conventional approaches, it is nearly impossible to learn the internal field gradient distribution in multiple pore scale systems. We have devised a pulse sequence that allows us to resolve this problem and to be able to probe the internal field gradients semiquantitatively. This proposed scheme can also be extended to a 2D representation for the diffusion coefficients of pore fluids as a function of pore sizes, allowing identification of pore fluids based on the contrast of their diffusion coefficients.

II. DIFFUSION IN POROUS MEDIA

The governing equations for diffusion of spins in a fluid medium is given by Torrey [2]:

$$\frac{\partial m_x}{\partial t}=\gamma(\mathbf{m}\times\mathbf{B}_0)_x-\frac{m_x}{T_2}+\boldsymbol{\nabla}\cdot D\boldsymbol{\nabla}m_x, \tag{2.1}$$

$$\frac{\partial m_y}{\partial t}=\gamma(\mathbf{m}\times\mathbf{B}_0)_y-\frac{m_y}{T_2}+\boldsymbol{\nabla}\cdot D\boldsymbol{\nabla}m_y, \tag{2.2}$$

$$\frac{\partial m_z}{\partial t}=\gamma(\mathbf{m}\times\mathbf{B}_0)_z-\frac{(m_z-m_0)}{T_1}+\boldsymbol{\nabla}\cdot D\boldsymbol{\nabla}m_z, \tag{2.3}$$

where γ is the gyromagnetic ratio, $\mathbf{B}_0$ is the magnetic field along the z axis, $\mathbf{m}$ is the density of unrelaxed spins, m_0 is the equilibrium magnetization, T_1 and T_2 are the longitudinal and transverse relaxation times, respectively, and D is the diffusion coefficient of the spins in the fluid. Here, we also omit the drift terms mentioned in Torrey's paper.

To consider the transverse component for a fluid-saturated porous medium, we introduce $m^+=m_x+im_y$, and the boundary condition at the surface/fluid interface. Equations (2.1) and (2.2) become

$$D\boldsymbol{\nabla}^2m^+(\mathbf{r},t)-\frac{m^+(\mathbf{r},t)}{T_{2B}}-i\gamma B_0(\mathbf{r})m^+(\mathbf{r},t)=\frac{\partial m^+(\mathbf{r},t)}{\partial t}$$

$$\hat{\mathbf{n}}\cdot D\boldsymbol{\nabla}m^+(\mathbf{r},t)+\rho m^+(\mathbf{r},t)|_S=0, \tag{2.4}$$

where ρ is the relaxation rate at the solid/fluid interface, or surface relaxation strength, T_{2B} is the bulk transverse relaxation time, and $\hat{\mathbf{n}}$ is the unit outward normal on the solid/fluid interface (i.e., it points out of the pore space into the solid matrix). The subscript "S" indicates the surface boundary condition [3].

In a reference frame rotating at the Larmor frequency, the precession term, $-i\gamma B_0(\mathbf{r})m^+(\mathbf{r},t)$, is replaced by

$-i\gamma(\mathbf{g}\cdot\mathbf{r})m^{+}(\mathbf{r},t)$, where $\mathbf{g}$ is the field gradient. For a perfectly homogeneous field, Eq. (2.4) reduces to the following in the rotating frame:

$$D\nabla^2 m^{+}(\mathbf{r},t)-\frac{m^{+}(\mathbf{r},t)}{T_{2B}}=\frac{\partial m^{+}(\mathbf{r},t)}{\partial t},$$

$$\hat{\mathbf{n}}\cdot D\nabla m^{+}(\mathbf{r},t)+\rho m^{+}(\mathbf{r},t)|_S=0. \tag{2.5}$$

When the surface relaxation strength is reasonably strong (i.e., $\rho\sim10\ \mu$m/s), the spins can only diffuse a short distance of a few pores, the spins at each pore relax more or less independently of the spins in other pores in a diffusion decoupled situation. The transverse component of the total magnetic moment of the fluid-saturated porous system, $M(t)=\int m^{+}(\mathbf{r},t)d^3\mathbf{r}$, can be expressed as

$$\frac{M(t_i)}{M_0}=\sum_j f_j e^{-t_i/T_{2j}}, \tag{2.6}$$

where t_i is the decay time for the ith echo in a Carr-Purcell-Meiboom-Gill (CPMG) [4,5] experiment, and f_j is the volume fraction of the pores characterized by a common T_2 relaxation time T_{2j}. Since $1/T_{2j}=\rho S_j/V_j$ (where S_j is the pore surface area and V_j is the pore volume) is the lowest eigenvalue of the solution for Eq. (2.5) when there is no magnetic field gradient, we have $T_{2j}=a_j/\rho$ with $a_j\equiv V_j/S_j$ as a measure of the size of the pore. Thus, the T_2 distribution (i.e., f_j vs T_{2j}) reflects the pore size distribution of the rock.

III. T_2 RELAXATION IN MAGNETIC FIELD GRADIENTS

If there is magnetic field gradient, the situation becomes somewhat complicated. For an *infinite* fluid medium, the first part of Eq. (2.4) can be solved [2] to show that there is an additional T_2 decay factor for the echo tops of a CPMG echo train, given by

$$\exp(-\gamma^2 g^2\tau^2 D t_i/3), \tag{3.1}$$

where γ is the gyromagnetic ratio, g is the magnetic field gradient, τ is the time between the $\pi/2$ and π pulses in a CPMG experiment, and D is the self-diffusion coefficient of the pore fluid. Here we have assumed near on-resonance condition and the rf pulse is perfect. At off-resonance condition with imperfect rf pulses in CPMG, the evolution of spin magnetization can be divided into different coherent pathways and the decay of the spin magnetization along each coherent pathway is different. However the echo train decay, averaged over all coherent pathways, still follows Eq. (3.1), i.e., the enhanced relaxation rate is proportional to τ^2 [6].

For a fluid-saturated porous medium in a magnetic field gradient, the problem becomes very complicated, and Eq. (2.4) cannot be solved easily [1]. The magnetic field inhomogeneities can come from an externally applied field gradient which is uniform over the pore scale, and/or from local field gradients that have a spatial variation at the pore scale. The latter is caused by the magnetic susceptibility contrast between the solid matrix and pore fluid. These gradients are affected by the pore shapes and sizes. There is no simple expression that would allow us to correlate internal field gradients and T_2 relaxation to experimental measurements.

However, if the diffusion time is short enough, we may assume that most of the spins have not experienced the existence of the pore wall and that the free diffusion formula for enhanced T_2 relaxation, i.e., Eq. (3.1), is still valid. In fact, the conditions for the validity of such an approximation has been discussed for a periodic system recently [7]. When significant number of spins start to experience the presence of the pore wall, the restricted diffusion may reduce the spin dephasing effect and hence the enhancement of the T_2 relaxation. As long as the Gaussian approximation for the phase distribution of the spins is satisfied, the restricted diffusion effect can be taken into account by using a time-dependent restricted diffusion coefficient. As the diffusion time becomes longer, eventually the Gaussian approximation breaks down and the free diffusion formula is no longer valid.

In the following discussion, we shall assume that the Gaussian approximation is valid. We shall later discuss the validity of such assumption in the last section. If the free diffusion formula is valid, we further assume that such enhanced T_2 relaxation can be integrated in a piecewise manner:

$$f_j e^{-t_i/T_{2j}}\int_j P_j(g)\exp[-\gamma^2 g^2\tau^2 D t_i/3]dg, \tag{3.2}$$

where $P_j(g)$ is the volume fraction within that size pores which have a gradient value of g, and

$$\int_j P_j(g)dg=1$$

is normalized to 1.

This piecewise integration would be appropriate if the diffusion time, i.e., τ, is infinitesimal. As the diffusion time increases, the piecewise integration with a true internal field gradient tends to produce a larger degradation than the true decay of the signal. The restricted diffusion effect of the pore walls also tends to reduce the signal decay. However, depending on the pore sizes and shapes, it is a complicated time-dependent evolution.

For now if we neglect all those intricacies, the challenge is to invert the CPMG data of variable echo spacings and be able to learn something about the internal field gradient distribution $P_j(g)$. The internal field gradients obtained this way would be the *apparent* field gradients. They would not be the *true* field gradients for the following reasons: (1) the inversion is done based on g^2 rather than $\mathbf{g}$, (2) there will be restricted diffusion effect, and (3) there will be field averaging effect where g varies rapidly, because only the cumulative change in the phase of the spins during the diffusing time is reflected in the inverted field gradients. We soon found that even with such qualifications, it is extremely difficult to analyze the CPMG data of variable echo spacing and be able to obtain the apparent internal field gradient distribution as a function of pore size.

IV. PREVIOUS EXPERIMENTAL ATTEMPTS

Early attempts [8–13] to quantify such internal field gradient distributions in rocks using the T_2 relaxation data obtained by the CPMG pulse sequence were largely unsuccessful. This is because they were limited by the regular CPMG data and were not able to decouple the integral of the internal field gradient term from the summation of the various pore sizes. To illustrate this, we note that the spin echo amplitudes of a CPMG echo train for fluid-saturated porous rock with internal gradients can be described as

$$\frac{M(t_i)}{M_0}=\sum_j f_j e^{-t_i/T_{2j}}\int_j P_j(g)\exp[-\gamma^2 g^2 \tau^2 D t_i/3]dg. \tag{4.1}$$

Here, for simplicity, we focus only on the problem of internal field gradient, and assume that externally applied field gradient is zero. In addition to the earlier assumption that the Gaussian approximation is valid, we further assume: (1) the internal field gradient distributions of pores of the same size are the same, and (2) the volume integral of the enhanced T_2 relaxation, i.e., $\exp(-\gamma^2 g^2 \tau^2 D t_i/3)$, over a range of possible gradient value g within a pore is quite close to the true attenuated spin echo amplitude, i.e., the field averaging effect is minimal.

Suppose we now collect a series of CPMG data, each with a different τ, and attempt to invert the internal field gradient distribution of the porous system from this set of data. The common approach [9,13] is to normalize all CPMG data with the one of the smallest τ:

$$\frac{M(t_i,\tau)}{M(t_i,\tau_s)}=\frac{\sum_j f_j e^{-t_i/T_{2j}}\int_j P_j(g)\exp[-\gamma^2 g^2 \tau^2 D t_i/3]dg}{\sum_j f_j e^{-t_i/T_{2j}}\int_j P_j(g)\exp[-\gamma^2 g^2 \tau_s^2 D t_i/3]dg} \tag{4.2}$$

where τ_s is the smallest τ. If there is only one dominant pore size, or $P_j(g)$ is the same for all pore sizes, then the integral in the numerator can be factored out. The summation over different pore sizes can be canceled, leaving Eq. (4.2) with a set of decaying data on the left-hand side and the integral of internal field gradients on the right-hand side,

$$b_i=\frac{M(t_i,\tau)}{M(t_i,\tau_s)}=\int_j P_j(g)\exp[-\gamma^2 g^2 \tau^2 D t_i/3]dg. \tag{4.3}$$

Then the internal field gradient distribution for the dominant pore size can be obtained through linear inversion using regularized routines.

This approach works when there is only one dominant pore size, and is incapable of deducing internal field gradient distributions for all pore sizes. The problem lies in the fact that it is difficult to decouple the integral of internal field gradients from the summation over the pore sizes. If an inversion is carried out when there are multiple pore sizes, the inverted internal field gradient distribution would be a strange composite of contributions from all pore sizes with very ambiguous physical meaning.

Suppose we are to tackle the problem in a two-dimensional fashion in the following manner: Invert the CPMG echo trains and obtain all T_2 distributions with different echo spacings. Display all these T_2 distributions as a function of echo spacing along a dimension perpendicular to the T_2 relaxation time axis. Presumably, one would expect that the T_{2j} amplitude decays along the dimension of increasing echo spacing similar to something like the following:

$$f_j\int_j P_j(g)\exp[-\gamma^2 g^2 D \tau^2/3]dg, \tag{4.4}$$

where we temporarily leave out the factor t_i in the exponent. Then, for each T_{2j} (or each pore size), we would be able to invert an internal field gradient distribution from this set of data with varying echo spacing. The result would then be a 2D plot of internal field gradient distribution as a function of T_{2j}, or pore size. Unfortunately, this scheme would not work. With the regular CPMG data of different τ's, the inversion routines would not give us a T_2 distribution with $f_j\int_j P_j(g)e^{-\gamma^2 g^2 D\tau^2/3}dg$ as an attenuated amplitude at T_{2j} for increasing τ, but rather, push the amplitude to a lower relaxation time, rendering it impossible to invert the internal field gradient distribution as a function of pore size. This is because the t_i in the exponent inside the integral $\int_j P_j(g)e^{-\gamma^2 g^2 D\tau^2 t_i/3}dg$ is not separable from the echo train, and the inverted T_{2j} amplitude would not be given as Eq. (4.4).

V. MODIFIED CPMG SEQUENCE

We have devised a modified CPMG sequence which allows us to resolve this problem. As shown in Fig. 1, we split a regular CPMG into two parts and run a 2D experiment. We use the smallest τ in the second part of the sequence such that the diffusion effect is minimized. In the first part of the sequence, τ is varied from the smallest to the largest values allowed. If the time window for the first part is t_0, the ith echo received in the second part of the sequence can be written as

$$b_{li}=\sum_{j=1}^{N_R} f_{lj}\exp[-(t_0+t_i)/T_{2j}]+\epsilon_i,$$
$$i=1,\ldots,N_E,\quad l=1,\ldots,N_\tau, \tag{5.1}$$

where N_R is the number of T_2 relaxation times equally spaced on a logarithmic scale preselected for the inversion, N_E is the number of echoes acquired in the second part of the sequence, N_τ is the number of different τ's, b_{li} is the ith echo of the lth τ measurement, ϵ_i is the noise for the ith echo, and f_{lj} the signal intensity associated with the relaxation time T_{2j} of the lth τ measurement and can be further decomposed to

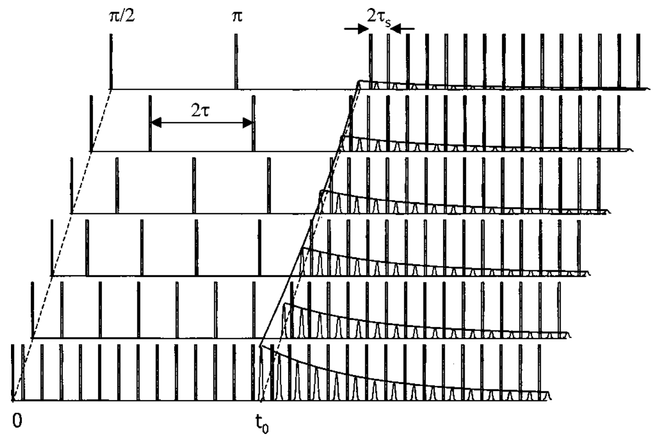

FIG. 1. The modified CPMG experiment where the pulsing sequence is split into two parts. The first part has a window width of t_0 where the echo spacing is varied from the smallest to the largest τ allowed, and the diffusion effect is encoded in the amplitudes corresponding to different relaxation times. Such information is collected in the second part of the pulse sequence using the regular CPMG and the smallest τ.

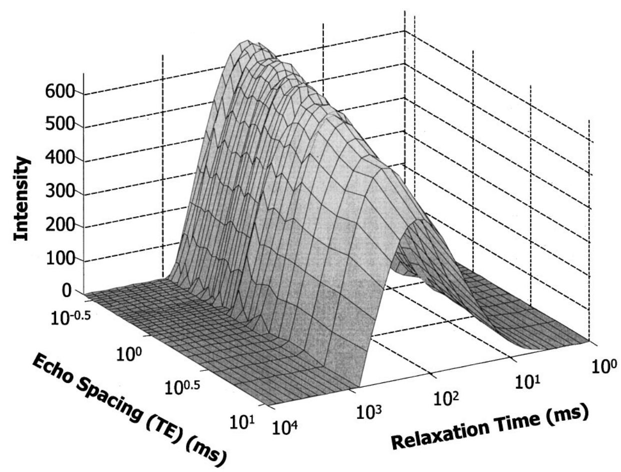

FIG. 2. The T_2 distributions inverted from the CPMG data collected in the second part of the modified sequence shown in Fig. 1, with various τ's used in the first part of the sequence. As τ (or echo spacing, time between echos is 2τ) increases, all T_2 amplitudes show a monotonically decreasing behavior due to diffusion effect.

$$f_{lj}=f_j^0\sum_{k=1}^{N_g} P_{jk}\exp[-\gamma^2 g_k^2\tau_l^2 D t_0/3]+\epsilon_l,$$

$$j=1,\ldots,N_R,\quad l=1,\ldots,N_\tau, \tag{5.2}$$

where N_g is the number of gradient components, g_k is a set of preselected gradient components equally spaced on a logarithmic scale, N_R is the number of relaxation times, f_j^0 is the unattenuated pore volume fraction having a relaxation time T_{2j} (i.e., f_{lj} when $\tau\rightarrow 0$, or the smallest τ), and P_{jk} is the normalized volume fraction that has a gradient value of g_k in the pore having a relaxation time T_{2j}. The P_{jk} matrix gives the 2D correlation distribution between the pore sizes and the internal gradients. It is the discretized form of $P_j(g)$ in Eq. (4.1).

Now that all echo trains are obtained with the same smallest τ, there is no problem in inverting them, and the T_2 distributions we obtain would not be shifted to shorter relaxation times, but instead, all information of the attenuation of the signal due to diffusion with different τ's within the window of t_0 is contained in f_{lj}, which is proportional to the following:

$$f_j^0\int_j P_j(g)\exp[-\gamma^2 g^2 D\tau_l^2 t_0/3]dg.$$

Here t_0 is a constant, and is decoupled from the echo train measured in the second part of the sequence. This allows our initial thought on the two-dimensional scheme to work properly.

VI. EXPERIMENTS AND DATA ANALYSIS

Figure 2 shows the results of CPMG measurements for a water-saturated sandstone using a MARAN ULTRA 2 MHz spectrometer. The detecting nuclei are hydrogen, and their resonance frequency is about 2 MHz. A t_0 of 10.4 ms was chosen for the first part of the sequence. The echo spacing varies from 0.26 to 10.4 ms within the first part of window t_0, whereas the smallest echo spacing, i.e., 0.26 ms was used for the second part. The 90° and the 180° pulses were 8.2 and 16.3 μs, respectively. The wait time was 2 s, and a total of 3072 echoes were acquired in the second part of the sequence. The signals were stacked 32 times with standard four phase cycling to improve the signal to noise ratio.

As shown in Fig. 2, a series of T_2 distributions inverted from CPMG echo trains of different τ's was plotted along the time-between-echoes axis, going from the smallest to the largest echo spacing. At each relaxation time T_{2j}, the amplitude f_{lj} is more or less monotonically decreasing as a function of the increasing τ_l, showing the enhanced relaxation due to diffusion effect from $e^{-\gamma^2 g^2 \tau_l^2 D t_0/3}$.

The inversion to get P_{jk} can be accomplished by a two-step process, solving Eq. (5.1) and then Eq. (5.2), by using the singular value decomposition method [14] and selecting proper cutoff of singular values commensurate with the noise level. However, if the τ values are not properly sampled, the error of the first inversion can seriously affect the accuracy of the second inversion. To minimize the error due to inversion, a one-step global inversion process can be implemented by merging Eqs. (5.1) and (5.2) and solving P_{jk} directly. Such a process creates a very large matrix and takes long iterative computations to obtain the result. Initial tests show that both one- and two-step inversions give similar results if the τ values are properly sampled within the window of t_0 and the inversion error is minimized.

The computation efficiency can be significantly improved by solving f_j^0 first using Eq. (5.1) and the data with the smallest τ, and removing those columns where f_j^0's are zero. This process alleviates a lot of grief because sometimes the value of $e^{-t_0/T_{2j}}$ can be so small that it reaches the limit of

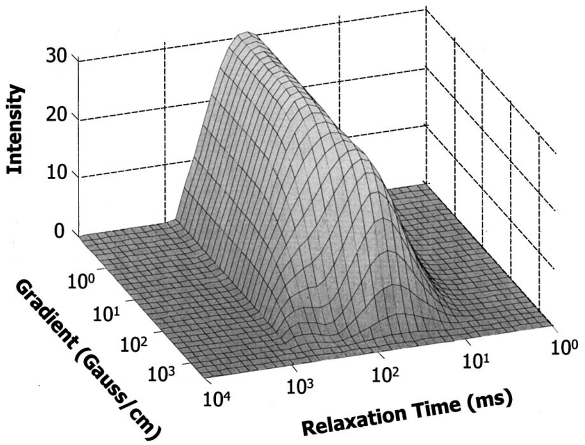

FIG. 3. The 2D plot of the internal field gradient distributions for different T_2 relaxation times (pore sizes) for a sandstone sample with moderate paramagnetic impurities, where the vertical amplitude is proportional to the proton population.

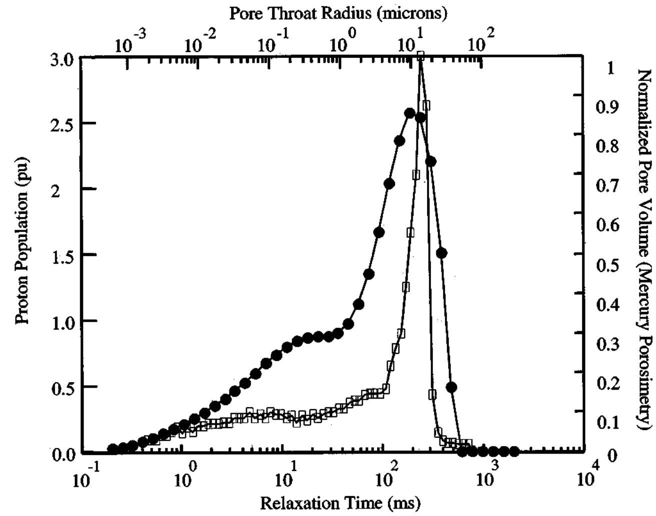

FIG. 5. The mercury porosimetry measurement (open squares) overlays on top the T_2 distribution (solid circles) of the sandstone sample analyzed in Fig. 3.

precision of the computer, causing problems in the inversion.

Figure 3 shows an example of a water-saturated sandstone where moderate paramagnetic impurities are present. The experimental conditions are the same as those in Fig. 2. The 2D plot displays the signal intensity (i.e., the vertical amplitude, or z axis, which is proportional to the proton population) as a function of T_2 relaxation times along one axis (different pore sizes) and internal field gradients along the other axis in the xy plane, both in logarithmic scale. The cross-sectional view at a fixed T_{2j} is the internal field gradient distribution for that relaxation time (or pore size). The integration along the gradient axis at a fixed T_{2j} gives the T_2 amplitude at that relaxation time. The total volume integral of the 2D plot gives the porosity of the rock.

Figure 4 shows another example of a sandstone. The experimental conditions were slightly different from those for Figs. 2 and 3. The window t_0 was about 10.2 ms, and the echo spacing varies from 0.34 to 10.2 ms for the first part of the sequence. For the second part of the sequence, the echo spacing was 0.17 ms, the wait time was 1 s, and a total of 6144 echoes were acquired. This sample has a bimodal T_2 distribution, with the small pores centered around 20 ms and the large pores centered around 150 ms. It is interesting to note that the small pores have a dominant peak of high internal field gradients.

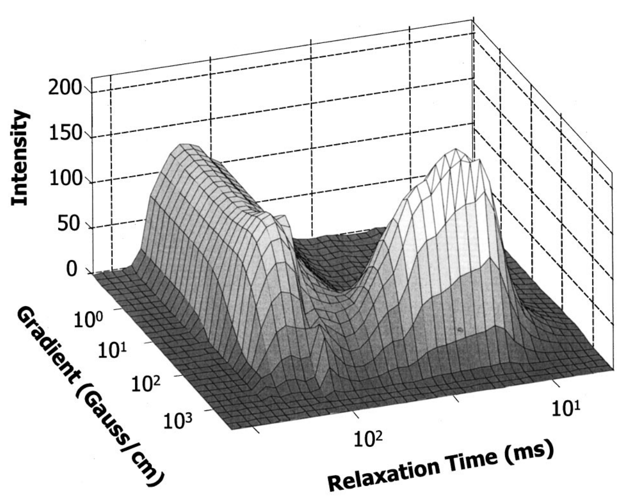

FIG. 4. The 2D plot of the internal field gradient distributions for different T_2 relaxation times (pore sizes) for another sandstone sample with significant paramagnetic impurities, where the vertical amplitude is proportional to the proton population.

VII. DISCUSSION

From this two-dimensional approach, we can gain much insight into the environment of the pore space or even the physical properties of the pore fluids in the rocks. Naturally, we have made several assumptions and/or approximations in our analysis. We should be aware of these limitations, and treat the results of the analysis as such.

We have assumed that different T_2 relaxation times truly reflect the pore size variations. This is a reasonably good approximation for sandstones where the surface relaxivity is strong. We have performed mercury porosimetry measurements for the sandstone samples used in Figs. 3 and 4 to corroborate this, and the results are shown in Figs. 5 and 6, respectively. The T_2 distributions are shown as solid circles and the mercury porosimetry results as open squares. Even though the former measures the pore body whereas the latter measures the pore throat, the correspondence between the two is excellent, indicating that the T_2 relaxation time reflects the pore size. A quick computation using a cylindrical pore model [i.e., $\rho_2 \sim r/(2T_2)$] shows that the surface relaxivity for the sandstone sample in Fig. 3 is around 30 μm/s and that in Fig. 4 around 17 μm/s.

Using a magnetic susceptibility balance (Johnson Matthey, MKII), we also measured the magnetic susceptibility of the solid grains of the sandstone samples used in Figs. 3 and 4. For the sample used in Fig. 3, $\chi_m \sim 11.4 \times 10^{-6}$ emu.

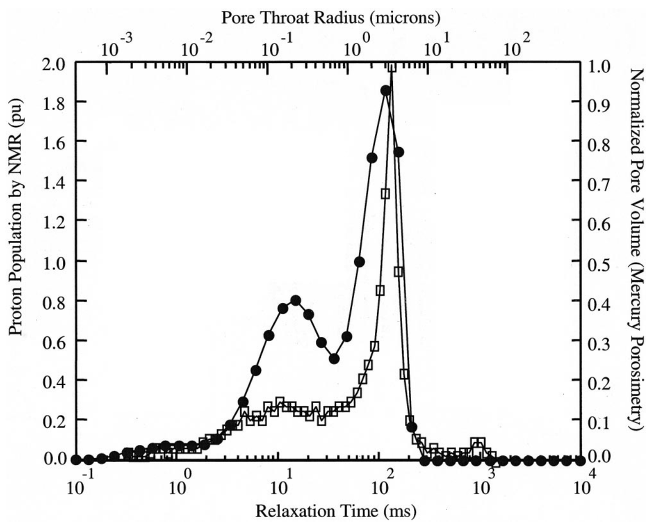

FIG. 6. The mercury porosimetry measurement (open squares) overlays on top of the T_2 distribution (solid circles) of the sandstone sample analyzed in Fig. 4.

Since χ_p for the pore fluid (i.e., water) is about -0.72×10^{-6} emu, $\Delta\chi \sim 12\times 10^{-6}$ emu. Using $g_{\mathrm{eff}} \approx B_0 \Delta\chi/a$ and $a \sim 12$ μm (from Fig. 5), we estimate the average internal field gradient for the dominant pores for Fig. 3 to be 4.7 G/cm (Note $B_0 \sim 469.7$ G). This appears to be a reasonable value. Since the pore fluid continues to exist for size less than 0.1 μm. It is conceivable that the internal gradient can go up to several hundred G/cm.

For the sample used in Fig. 4, both T_2 and mercury porosimetry measurements show a clear bimodal pore size distribution. The magnetic susceptibility of the solid grains was measured to be 1.7×10^{-6} emu. The leads to a $\Delta\chi \sim 2.4 \times 10^{-6}$ emu. Using the dominant pore size of 3.5 μm, we estimate the average internal field gradient for that pore size to be 3.2 G/cm. If we use the smaller peak at 0.1 μm, we get an average internal field gradient for the small pores to be 113 G/cm. Considering the grains could have sharp corners, this value is quite reasonable when we look at the distinct bump in the field gradient distribution for the small pores in Fig. 4.

Even though the internal field gradients can be as high as several hundred to thousand G/cm, the experimental conditions are quite close to on-resonance condition, and we do not need to be concerned with the off-resonance condition discussed in the literature [6]. This is because the large gradients are mainly due to extremely small pore sizes. Using a maximum gradient of 1000 G/cm and a large pore dimension of 12 μm, the maximum ΔB_0 is about 1 G. Since the 90° pulse is 8.2 μs, this leads to a B_1 of 7.2 G. Thus, the on-resonance condition, $B_1 \gg \Delta B_0$, is satisfied.

Based on the previous model calculation on periodic porous system [7], our examples for Figs. 3 and 4 (the maximum diffusion time in both cases is $\tau \sim t_0/2 \sim 5$ ms), when using the dominant pore size as an estimate, are within the limit of the validity of Gaussian approximation. Thus for smaller pores, the Gaussian approximation may be violated. Furthermore, the diffusion coefficient for water may be reduced due to restricted diffusion effect. Both effects would tend to produce an apparent internal field gradients smaller than they really are, especially for small size pores.

There are also limitations in the inversion schemes. Both Figs. 3 and 4 were obtained using a two-step process. The detailed 2D-plot features near small field gradients depend on the selection of t_0. When a short t_0 is used, we are able to recover more short T_2 components. Also, the large field gradient features (usually occur at short T_2 components) can be extracted because the diffusion effects would be significant. However, the low field gradient features for large pores will not have significant variations for a small t_0. This explains the flat and smooth distribution shown at low gradient values for large pores in both Figs. 3 and 4. On the other hand, if the t_0 is too long, we will lose the short T_2 components altogether. For both Figs. 3 and 4, a t_0 about 10 ms was chosen, which is probably not long enough to elucidate the low field gradient features for large pores. However, one has to be concerned with the validity of Gaussian approximation. A t_0 much larger than 10 ms would violate this assumption.

Characterizing the apparent internal field gradient distribution, induced by the magnetic susceptibility contrast between the solid matrix and pore fluid, as a function of pore size is an interesting problem. A well developed 2D methodology, however, can have important practical implications. Similar scheme can be applied to obtain a 2D plot with the T_2 relaxation time as one axis and the diffusion coefficient of pore fluids as the other axis. This can be accomplished by using pulsed field gradients applied between π pulses during the first part of the 2D experiment within the window t_0. Because the pulsed field gradients are significantly larger than the background gradients, a good estimate of the distributed diffusion coefficients can be obtained from the inversion of a suite of measurements of different τ's. Or else, the distribution of internal field gradients can be obtained earlier and incorporated into the data analysis.

The result of this exercise will be a 2D plot with its vertical amplitudes being proportional to the proton population as a function of T_2 relaxation times (i.e., pore sizes) on one axis, and the diffusion coefficients (i.e., different pore fluids) on the other axis. The diffusion coefficient of oil is significantly different from that of water. Thus, it is possible to identify oil from water in this 2D plot. The viscosity of the oil can also be estimated. The investigation on this subject is ongoing, and the results shall be reported shortly.

The techniques for obtaining the distribution of diffusion coefficients need not be limited to the use of pulsed field gradients with varying τ. Other techniques, such as Tanner's stimulated echo technique [15] with varying diffusion time, pulsed field gradient, or pulse width have been shown to be successful in obtaining a distribution of diffusion coefficients [16].

VIII. CONCLUSION

In conclusion, we have demonstrated a two-dimensional scheme for analyzing NMR relaxation data using a devised modified CPMG pulse sequence. This technique allows us to produce a 2D plot of apparent internal field gradient distribution as a function of T_2 relaxation time, with one axis being the T_2 relaxation time, the other axis being the internal field gradient, and third axis being proportional to proton population.

Such 2D technique can be easily extended to other physical quantities such as diffusion coefficients or proton spectra of the pore fluids. The work of such investigation shall be reported elsewhere.

ACKNOWLEDGMENTS

The authors wish to thank Dr. John Popek for making the mercury porosimetry measurements, Simon Stonard and Bruce Bilodeau for helpful discussion, and Glenn Menard for the technical assistance. They also wish to thank the management of ChevronTexaco Exploration and Production Technology Company for the support of and the permission to publish this work.

[1] D.J. Bergman and K.-J. Dunn, Phys. Rev. E **52**, 6516 (1995).
[2] H.C. Torrey, Phys. Rev. **104**, 563 (1956).
[3] K.R. Brownstein and C.E. Tarr, Phys. Rev. A **19**, 2446 (1979).
[4] H.Y. Carr and E.M. Purcell, Phys. Rev. **94**, 630 (1954).
[5] S. Meiboom and D. Gill, Rev. Sci. Instrum. **29**, 668 (1958).
[6] M.D. Hürlimann, J. Magn. Reson. **148**, 367 (2001).
[7] K.-J. Dunn, Magn. Reson. Imaging **19**, 439 (2000).
[8] P. Bendel, J. Magn. Reson. **86**, 509 (1990).
[9] M.D. Hürlimann, J. Magn. Reson. **131**, 232 (1998).
[10] M. Appel, J.J. Freeman, R.B. Perkins, and J.P. Hofman, in Proceedings of the 40th Annual Logging Symposium of the Society of Professional Well Log Analysts, Oslo, Norway, 1999 (unpublished), Paper FF.
[11] J.L. Shafer, D. Mardon, and J. Gardner, in Symposium Proceedings of the Society of Core Analysts, Golden, CO, 1999 (unpublished), Paper 9916.
[12] G.Q. Zhang, G.J. Hirasaki, and W.V. House, in Proceedings of the 41st Annual Symposium of the Society of Professional Well Log Analysts, Dallas, TX, 2000 (unpublished), Paper AA.
[13] K.-J. Dunn, M. Appel, J.J. Freeman, J.S. Gardner, G.J. Hirasaki, J.L. Shafer, and G. Zhang, in Proceedings of the 42nd Annual Symposium of the Society of Professional Well Log Analysts, Houston, TX, 2001 (unpublished), Paper AAA.
[14] K-J. Dunn and G.A. LaTorraca, J. Magn. Reson. **140**, 153 (1999).
[15] J.E. Tanner, J. Chem. Phys. **52**, 2523 (1970).
[16] S.-W. Lo, G.J. Hirasaki, W.V. House, and R. Kobayashi, in Proceedings of the Society of Petroleum Engineers, Dallas, TX, 2000 (unpublished), SPE Paper 63217.